2009

Singular Superposition/Boundary Element Method for Reconstruction of Multi-dimensional Heat Flux Distributions with Application to Film Cooling Holes

Mahmood Silieti
University of Central Florida

Eduardo Divo
Embry-Riddle Aeronautical University, Eduardo.divo@erau.edu

Alain J. Kassab
University of Central Florida, Alain.Kassab@ucf.edu

Scholarly Commons Citation

Silieti, M., Divo, E., & Kassab, A. J. (2009). Singular Superposition/Boundary Element Method for Reconstruction of Multi-dimensional Heat Flux Distributions with Application to Film Cooling Holes. *Computers, Materials & Continua, 12*(2). https://doi.org/10.3970/cmc.2009.012.121

 CMC, vol.12, no.2, pp.121-143, 2009

Singular Superposition/Boundary Element Method for Reconstruction of Multi-dimensional Heat Flux Distributions with Application to Film Cooling Holes

Silieti, M.[1], **Divo, E.**[2] **and Kassab, A.J.**[1]

Abstract: A hybrid singularity superposition/boundary element-based inverse problem method for the reconstruction of multi-dimensional heat flux distributions is developed. Cauchy conditions are imposed at exposed surfaces that are readily reached for measurements while convective boundary conditions are unknown at surfaces that are not amenable to measurements such as the walls of the cooling holes. The purpose of the inverse analysis is to determine the heat flux distribution along cooling hole surfaces. This is accomplished in an iterative process by distributing a set of singularities (sinks) inside the physical boundaries of the cooling hole (usually along cooling hole centerline) with a given initial strength distribution. A forward steady-state heat conduction problem is solved using the boundary element method (BEM), and an objective function is defined to measure the difference between the heat flux measured at the exposed surfaces and the heat flux predicted by the BEM under the current strength distribution of the singularities. A Genetic Algorithm (GA) iteratively alters the strength distribution of the singularities until the measuring surfaces heat fluxes are matched, thus satisfying Cauchy conditions. The distribution of the heat flux at the walls of the cooling hole is determined in a post-processing stage after the inverse problem is solved. The advantage of this technique is to eliminate the need of meshing the surfaces of the cooling holes, which requires a large amount of effort to achieve a high quality mesh. Moreover, the use of singularity distributions significantly reduces the number of parameters sought in the inverse problem, which constitutes a tremendous advantage in solving the inverse problem, particularly in the application of film cooling holes.

[1] Mechanical, Materials, and Aerospace Engineering, University of Central Florida
[2] Department of Engineering Technology, University of Central Florida

1 Introduction

Given the large number of sustained operational hours required for industrial turbines, two important demands placed on such engines are component life and overall engine performance. These demands are somewhat conflicting because high temperatures are required at the inlet to the turbine in order to achieve high efficiency, however, increasing turbine inlet temperature in turn causes reduced component life. One way to overcome this problem is to employ film cooling. Film cooling is the introduction of a secondary fluid (coolant or injected fluid) at one or more discrete locations along a surface exposed to a high temperature environment to protect that surface not only in the immediate region of injection but also in the downstream region [Goldstein (1971)]. To define film cooling effectiveness (η), the surface temperature downstream of the cooling hole has to be measured or computed. An expression is often used for compressible flow film cooling [Goldstein (1971)] is:

$$\eta = \frac{T - T_r}{T_{oc} - T_r} \tag{1}$$

Here, T is the measured temperature downstream of the cooling hole, T_{oc} is the stagnation temperature of the cooling fluid at the point of injection, and T_r is the recovery temperature of the hot gas. The recovery temperature can be defined as the fluid bulk temperature, or the adiabatic wall temperature. It is important to characterize the efficacy of such a cooling scheme, particularly as the compressor air employed to protect critical parts of the turbine is very expensive from an overall engine performance perspective. The film effectiveness is a common way to report the adiabatic wall temperature that is the driving temperature for the convection at the exposed metal surfaces and to simultaneously provide a measure of the efficacy of film cooling scheme. The film effectiveness can be measured in carefully designed experiments. However, in determining the film coefficient distributions at the exposed surfaces, the distributions of thermal conditions within the cooling holes are unknown. As there are no correlations or experimental data in the open literature available to characterize an accurate heat flux distribution in such cases, there exists a need to determine the film coefficient distributions in a film cooling holes.

Film cooling configurations have been investigated for several years. Concerning the CFD research on this subject, a bibliography (1971-1996) of the most important publications can be found in a study by Kercher [Kercher (1998)]. On the three-dimensional film cooling side, most of the published work on predictions of film cooling is based on either a parabolic or semi elliptic procedure. Goldstein et al.

[Goldstein et al (1974), Goldstein at al (1998)] studied the effect of cooling holes on turbine vanes and blades. Recent numerical studies on the leading edge film cooling physics [York and Lylek (2002)] focused on the determination of the adiabatic film cooling effectiveness and heat transfer coefficients.

In several industrial applications, it is necessary to accompany the computation of the flow and associated heat transfer in the fluid with the heat conduction inside the adjacent solid surfaces. The coupling of these two modes of heat transfer is termed as conjugate heat transfer (CHT) in the literature. Several researchers have investigated coupled conjugate heat transfer analysis. Some of them presented a coupled scheme between finite volume based Navier-Stokes solver and a finite element based program for heat conduction [Heselhaus and Vogel(1995)], others used finite volume based code Fluent version 5.0 [York and Lylek (2003)] and Fluent version 6.0 [Silieti et al (2004)], whereas others pursued a different method of coupling the fluid and solid thermal problems. The basis for their technique is the boundary element method (BEM) for the solution of solid conduction problem. Since the thermal conduction in the solid is governed by Laplace equation for temperature, it may be solved using only boundary discretization [Kasab et al (2003)].

Retrieval of the distribution of surface heat flux or convective heat transfer coefficient (h) is often accomplished using surface temperature histories provided by thermographic techniques applied in controlled experiments, and, in conjunction with theoretical assumptions. It is herein proposed to use the boundary elements method (BEM) to resolve three-dimensional heat transfer and to determine (h) by inverse methods. The BEM is ideally suited for this inverse problem as surface temperatures and fluxes appear as nodal unknowns. Surface fluxes have been retrieved using BEM-based inverse algorithms and internal temperature measurements. In earlier studies the authors [Kassab etl (1999), Divo et al (1999), Silieti al (2004 and 2009)] developed an inverse algorithm to reconstruct multi-dimensional surface heat flux distribution, and minimized the functional using the Levenberg-Marquardt method and GAs. They showed that GAs can be used successfully to retrieve surface heat flux distributions. Divo et al. [Divo et al (2003 and 2004)] developed a method relying on a superposition of clusters of sources/sinks with a boundary element solution of the forward problem to solve the inverse geometric problem of detection of subsurface cavities and flaws using thermographic techniques. Silieti et al. [Silieti et al 2004] developed a hybrid singularity superposition/boundary element-based inverse technique to reconstruct heat flux distributions for the cases of one and two cooling slots. Their results validated the approach and revealed good agreement between the BEM/GA predicted heat fluxes and the CHT simulated heat fluxes along the inaccessible cooling slot walls.

In this paper, the technique developed by Silieti et al. [Silieti et al 2004] will be

adopted and extended to three-dimensional applications, and specifically to film cooling holes. In this technique the inlets and the exits of the cooling holes will be assigned an adiabatic boundary condition and a distribution of singularities (sinks) will be located inside the physical boundaries of each cooling hole (usually along cooling hole centerline) with a given initial strength distribution. A forward steady-state heat conduction problem will be solved using the boundary element method (BEM), and an objective function will be defined to measure the difference between the heat flux measured at the exposed surfaces and the heat flux predicted by the BEM under the current strength distribution of the singularities. A GA iteratively alters the strength distribution of the singularities until the measuring surfaces heat fluxes are matched, thus satisfying Cauchy conditions. Subsequent to the solution of the inverse problem, the heat flux at the inaccessible surfaces is computed using BEM. The distribution of the heat flux at the walls of the cooling hole is determined in a post-processing stage after the inverse problem is solved.

2 Singularity Superposition and Inverse Problem Methodology

Considering the case of a 3D film cooling hole supplied by a plenum, see Figure 1(a). The model consists of the hot gas domain, the coolant plenum supply (cold air), and the endwall with single square/circular cooling hole. The measured temperature and heat flux at overspecified surfaces (red color) are shown in Figure 1(b), will be used as an input for the inverse problem to determine the distributions of the temperature and heat flux along the film cooling hole walls. Also, the sides of the endwall in addition to the inlet and the exit surfaces of the cooling hole are set to be adiabatic.

The inverse problem algorithm developed herein is similar to the one developed in the previous study. Again, this methodology comprised of the forward problem solver: a hybrid singular superposition/BEM method, and an inverse problem solver: GA to determine strength distribution of the sinks to match Cauchy conditions imposed at exposed surfaces.

2.1 The Forward Problem Solver

The purpose of the inverse problem is to determine the heat flux distribution (q) at the walls of the cooling hole. This is accomplished in an iterative process. The temperature is imposed at the exposed surfaces (top/bottom surfaces of the endwall), and to simulate the extraction of energy from the coolant, a distribution of singularities (sinks) is located in the vicinity of the cooling hole surfaces within the hole physical domain with a given initial strength distribution, see Figure 2, usually, the sinks will be located along the cooling hole centerline. The inlet and

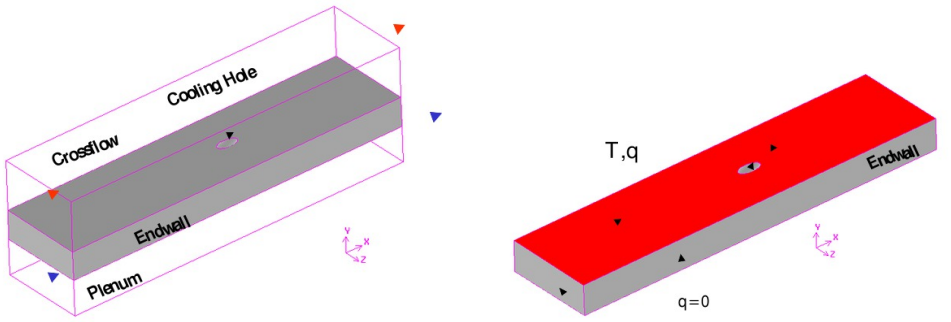

(a) overall configuration. (b) domain of the inverse conduction problem.

Figure 1: . Schematic diagram for the Inverse Problem.

the exit surfaces of the cooling hole will be insulated to prevent energy from flowing through them, this way all the energy that was extracted through the physical cooling surface is captured by the sinks.

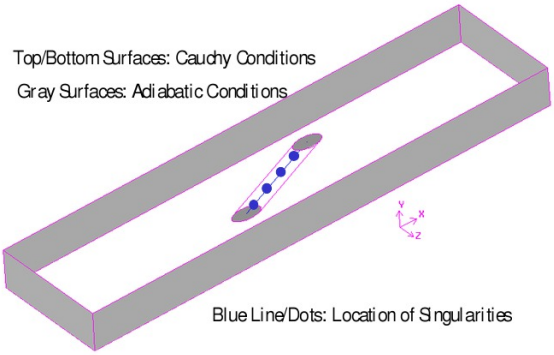

Figure 2: Thermal singularity superposition configuration.

The mathematical formulation that follows this idea consists of the Poisson equation for the temperature $T(x,y)$ where the generation term is the summation of singular field perturbations characterized by NS localized Dirac delta functions as:

$$\nabla.[k\nabla T(x,y,z)] + \sum_{K=1}^{NS} Q_K \delta(x,y,z,x_K,y_K,z_K) = 0 \tag{2}$$

where the generation term is the summation of singular field perturbations characterized by the number of singularities/sinks (NS) localized Dirac delta functions,

k is the thermal conductivity ($W/m.K$), Q_K represents the strength of the sinks, (x_K, y_K, z_K) represents location of the K^{th} sink, and δ is Dirac delta function. Again, the boundary elements method (BEM) approach is adopted to solve this problem. A standard BEM formulation starts with the introduction of an arbitrary function $G(x,y,z,x_i,y_i,z_i)$ and a transformation of the governing equation into an integral equation over the domain Ω as:

$$\int_\Omega \nabla.[k\nabla T(x,y,z)]G(x,y,z,x_i,y_i,z_i)d\Omega = \sum_{K=1}^{NS} Q_K \int_\Omega \delta(x,y,z,x_K,y_K,z_K)G(x,y,z,x_i,y_i,z_i)d\Omega \tag{3}$$

To transform the domain integral into contour integrals over the boundary (Γ); Green's second identity is applied on the left-hand side and the sifting property of the Dirac delta function is applied on the right-hand side of the equation above yielding:

$$\int_\Omega \nabla.[k\nabla G(x,y,z,x_i,y_i,z_i)]\,T(x,y,z)\,d\Omega + \oint_\Gamma H(x,y,z,x_i,y_i,z_i)\,T(x,y,z)\,d\Omega - \oint G(x,y,z,x_i,y_i,z_i)\,q(x,y,z)\,d\Gamma = \sum_{K=1}^{NS} Q_K\,G(x_K,y_K,z_K,x_i,y_i,z_i) \tag{4}$$

where:

$$H(x,y,z,x_i,y_i,z_i) = -k\,\partial G(x,y,z,x_i,y_i,z_i)/\partial n$$
$$q(x,y,z) = -k\partial T(x,y,z)/\partial n \tag{5}$$

Now, a Dirac delta function is used to perturb the adjoint operator on the arbitrary function $G(x,y,z,x_i,y_i,z_i)$ present in the last remaining domain integral in the equation as:

$$\nabla.[k\nabla G(x,y,z,x_i,y_i,z_i)] = -\delta(x,y,z,x_i,y_i,z_i) \tag{6}$$

For 3D problems $G(x,y,z,x_i,y_i,z_i)$ can be found as the free-space solution to the adjoint equation as:

$$G(x,y,z,x_i,y_i,z_i) = \frac{1}{4\pi k\sqrt{(x-x_i)^2+(y-y_i)^2+(z-z_i)^2}} \tag{7}$$

Again, the sifting property of the Dirac delta function is recasted to lead to the following boundary-only integral equation:

$$C(x_i,y_i,z_i)\ T(x_i,y_i,z_i) - \oint_\Gamma T(x,y,z)H(x,y,z,x_i,y_i,z_i)d\Gamma + \tag{8}$$
$$\oint_\Gamma q(x,y,z)\ G(x,y,z,x_i,y_i,z_i)d\Gamma = \sum_{K=1}^{NS} Q_K\, G(x_K,y_K,z_K,x_i,y_i,z_i)$$

Introducing boundary discretization yields the following relation:

$$C_i\ T_i - \sum_{j=1}^{N} \widehat{H}_{ij}\ T_j + \sum_{j=1}^{N} G_{ij}\ q_j = \sum_{K=1}^{NS} Q_K\, G(x_K,y_K,z_K,x_i,y_i,z_i) \tag{9}$$

where:

$$C_i = 1 \text{ if } (x_i,y_i,z_i) \in \Omega \tag{10}$$
$$C_i = \frac{1}{2} \text{ if } (x_i,y_i,z_i) \in \Gamma \text{ (smooth boundaries)}$$
$$C_i = 0 \text{ if } (x_i,y_i,z_i) \notin \Omega$$

Following the discretization of the boundary (Γ) with (N) nodal locations and the collocation of (x_i,y_i,z_i) at these (N) locations, the above equation reduces to the following simultaneous set:

$$\sum_{j=1}^{N} G_{ij}\, q_j - \sum_{j=1}^{N} H_{ij}\ T_j = S_i \tag{11}$$

where:

$$H_{ij} = \widehat{H}_{ij} - \frac{1}{2}\delta_{ij} \tag{12}$$
$$S_i = \sum_{K=1}^{NS} Q_K\, G(x_K,y_K,z_K,x_i,y_i,z_i)$$

In the problems reported herein we utilize constant boundary elements, and adaptive Gauss-Legendre quadratures with special treatment for the self influence coefficients were employed to evaluate the surface intergrals. Details of our 3D code (that also features discontinuous bilinear and biquadratic boundary elements) along with the quadrature and discretization procedures are provided in the monograph [Divo and Kassab (2003)] where the treatment of variable thermal conductivity both in terms of spatial variation and non-linear dependence on the temoperature

are treated in detail. In the case of temperature dependence alone, the problem can be treated via a Kirchhoff transformation [Divo et al (2003)], while in the case of heterogeneous dependence of the thermal conductivity (dependance on space), including anisotropy, a special Green's function has been devised to solve the heat conduction problem [Divo and Kassab (1997), Kassab and Wrobel (2000), Wrobel and Aliabadi(2002), Divo et al (2003)].

The strength of singularities can be estimated by carrying out an energy balance over the domain of the inverse problem (endwall) which yields to Equation (2), then integrating over the domain (Ω) yields the following relations:

$$\int_{\Omega} \nabla.[k\nabla T(x,y,z)]d\Omega + \sum_{K=1}^{NS} Q_K \int_{\Omega} \delta(x,y,z,x_K,y_K,z_K)d\Omega = 0 \tag{13}$$

$$\oint_{\Gamma} k\nabla T(x,y,z).\vec{n}d\Gamma + \sum_{K=1}^{NS} Q_K = 0 \tag{14}$$

$$-\oint_{\Gamma} q_n d\Gamma + \sum_{K=1}^{NS} Q_K = 0 \tag{15}$$

or,

$$\sum_{K=1}^{NS} Q_K = \oint_{\Gamma} q_n d\Gamma = \sum_{\Gamma_W} q_n A_{\Gamma_W} = \sum_{\Gamma_i} q_n A_{\Gamma i} \tag{16}$$

where A is the surface area of the each boundary, Γ_W are the wall boundaries of the cooling hole, and Γ_i are the surface boundaries for the domain of the inverse problem. Provided that a well-posed problem is conformed with a properly defined geometry and set of boundary conditions, see Figure 3, the discretized boundary integral equation, Equation. (11) is reduced to:

$$A_{ij}\, x_j = b_i + S_i \tag{17}$$

with $i = 1...N$ and where S_i contains the effects of the added singularities Q_K. The solution to this system provides the full distribution of temperatures and heat fluxes around the boundary that can later be used in the same formulation to calculate temperatures and heat fluxes any where in the domain Ω. Notice that the system in Equation (17) needs to be generated and LU- decomposed only once, and changing the strength of the singularities can be efficiently accounted for in the solution by just updating the right-hand side vector and solving the system again by a forward and back substitution.

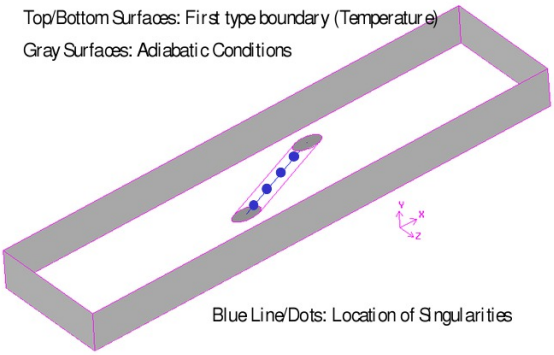

Figure 3: Set of boundary conditions for the BEM problem.

2.2 The Inverse Problem Solution

The purpose of the inverse problem is to determine the heat flux distributions at the surfaces/walls of the film cooling hole. This is done in an iterative process; the temperature is imposed at exposed surfaces (top/bottom surfaces) and a distribution of singularities (sinks) is located within the physical domain of the cooling hole (along cooling hole center line) with a given initial strength distribution. A forward steady-state heat conduction problem is solved using the boundary element method (BEM), and an objective function is defined to measure the difference between the heat flux measured at the exposed surfaces and the heat flux predicted by the BEM under current strength distribution of the sinks. This can be accomplished by minimizing the following least-squares functional:

$$S(Q_K) = \sqrt{\left(\sum_{i=1}^{N_m} R_i\right)\left(\frac{1}{N_m}\sum_{i=1}^{N_m}\frac{\left[q_i(Q_K)-\widehat{q}_i\right]^2}{R_i}\right)} \tag{18}$$

where N_m is the number of measuring points, $\widehat{q}_i$ are the measured heat fluxes at the measuring points, and $q_i(Q_K)$ are the computed heat fluxes for a given set of sink strengths, R_i is defined to measure the smallest distance between any element and the location of the singularities (sinks); i.e. R_i is equal to the minimum of either $R1_i$ or $R2_i$, where $R1_i$ and $R2_i$ are defined as follows:

$$\begin{aligned} R1_i &= (x_{ci}-x_{exit})^2+(y_{ci}-y_{exit})^2+(z_{ci}-z_{exit})^2 \\ R2_i &= (x_{ci}-x_{inlet})^2+(y_{ci}-y_{inlet})^2+(z_{ci}-z_{inlet})^2 \end{aligned} \tag{19}$$

where (x_{ci}, y_{ci}, z_{ci}) are the coordinates of the center of the *i-th* element, $(x_{inlet}, y_{inlet}, z_{inlet})$ is the physical center of the cooling hole inlet, and $(x_{exit}, y_{exit}, z_{exit})$ is the physical

center of the cooling hole exit. As we mentioned before that the inherent regularization property of the GA (minimization method of choice in this study), in addition to the discrete nature of a finite number of singularities (sinks) to simulate the extracted energy, makes it unnecessary to add any additional regularization to the functional, and would just slow down the minimization process. Once the functional, $S(Q_K)$, is minimized, the resulting heat flux distribution along the physical walls of the film cooling hole can be smoothed-out by simple least-squares means. Moreover, the calculation of the normal heat fluxes at the walls of the cooling hole (four lines, one line per side) is done at a post-processing stage by computing the heat flux vector components at internal points along the walls of the cooling hole (4-lines).

2.3 The Genetic Algorithm

The GA optimization process begins by setting a random set of possible solutions, called the population, with a fixed initial size or number of individuals. Each individual is defined by optimization variables and is represented as a bit string or a chromosome, see Figure 4. A GA iteratively alters the strength distribution of the singularities until the measuring surfaces heat fluxes are matched, thus satisfying Cauchy conditions at the exposed measuring surfaces. It should be noted that GA's maximize objective function as they naturally seek the "best fit" [Goldberg (1989)]. Thus the objective function computed by the GA is actually,

$$\mathrm{Z}_{GA}(Q_K) = S(Q_K)^{-1} \tag{20}$$

The objective function, $Z_{GA}(\tilde{q}_A)$, is evaluated for every individual in the current population defining the fitness or their probability of survival. At each iteration of the GA, the processes of selection, crossover, and mutation operators are used to update the population of designs. A selection operator is first applied to the population in order to determine and select the individuals that are going to pass information in a mating process with the rest of the individuals in the population. This mating process is called the crossover operator, and it allows the genetic information contained in the best individuals to be combined to form offsprings. Additionally, a mutation operator randomly affects the information obtained by the mating of individuals. This is a crucial step for continuous improvement.

A series of parameters are initially set in the GA code, which determine and affect the performance of the genetic optimization process. The number of parameters per individual or optimization variables, the size of the bit string or chromosome that defines each individual, the number of individuals or population size per generation, the number of children from each mating, the probability of crossover, and the probability of mutation are among the parameters that control the optimization pro-

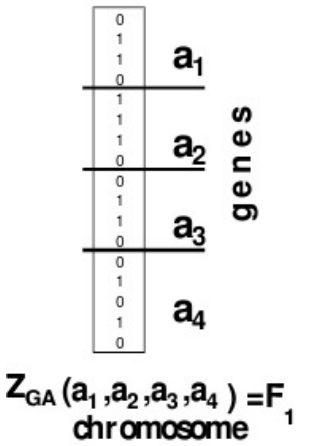

Figure 4: Example of an individual in the population characterized by four parameters (genes) encoded in a chromosome yielding the individual's fitness value F_1.

cess. This set of operations are carried out generation after generation until either a convergence criterion (a preset level of acceptable fitness) is satisfied or a maximum number of generations is reached. It is also important to point out that three important features distinguish GA from the other evolutionary algorithms, namely: (1) binary representation of the solution, (2) the proportional method of selection, and (3) mutation and crossover as primary methods of producing variations.

In nature, the properties of an organism are described by a string of genes in the chromosomes. Therefore, if one is trying to simulate nature using computers one must encode the design variable in a convenient way. We adopt a haploid model using a binary vector to model a single chromosome. The length of the vector is dictated by the number of design variables and the required precision of each design variable. Each design variable has to be bounded with a minimum and a maximum value. The haploid GA places all design variables into one binary string, called a chromosome or off-spring and the information contained in the string of vectors comprizing the chromosome characterizes an individual in a population. In turn, each individual is equipped with a given set of design variables to which corresponds a value of the objective function. This value is the measure of "fitness" of the individual design. In a GA, poorly fit designs are not discarded; rather they are kept, as in nature, to provide genetic diversity in the evolution of the population. This genetic diversity is required to provide forward movement of the population during the mating, crossover, and mutation processes which character-

ize the GA. Details of these operations can be found in the standard optimization literature [Goldberg (1989)]. The following suitable parameters were chosen to generate results: a population size of 50 individuals/generation, a string of eight bits to define each parameter within each individual. The mating process produces one child per mating using uniform crossover which produces a high level of diversity, a 4% probability of jump mutation, a 20% probability of creep mutation, and a 50% probability of crossover. The population is not allowed to grow (static population) and elitistic generation (the best parent survives to the next generation). The population is completely eliminated after 50 generations if there is no further improvement, keeping the best member of the population (restart). This combination of parameters and procedures has been proven to yield efficient and accurate optimization results for different cases carried out in this paper.

3 Numerical Results

Here, the results of the inverse problem will be presented for two cases: the results for single square cooling hole, and the results for single circular cooling hole. For the case of a square cooling hole, a forward problem is solved using the BEM to generate boundary conditions at the exposed surfaces (top/bottom surfaces), those are in turn were used to simulate inputs to the inverse problem. In contrast, for the case of the circular hole, a full conjugate heat transfer (CHT) model is developed to simulate the experimentally measured data at the exposed surfaces, which will provide a numerical input for the inverse problem.

3.1 Results of the Inverse Problem for Square Cooling Hole

First, a solution to the forward problem will be established to be used in obtaining heat flux measurements which serves as a numerical input to the inverse problem. In specific, consider a rectangular endwall $((x = 11cm)\times(y = 21cm)\times(z = 3cm))$ with a vertical square cooling hole located at the geometrical center of the endwall, the cross-sectional area of the cooling hole is $(1cm \times 1cm)$. The problem is discretized using $((Nx = 11)\times(Ny = 21)\times(Nz = 3))$ constant elements for the endwall and $((Nh = 1)\times(Nh = 1))$ for the cooling hole. The total number of elements is calculated according to the following relation:

$$N = 2(NxNy + NxNz + NyNz) + 4NzNh - 2NhNh \tag{21}$$

Based on the above relation the total number of elements for the direct problem is 664 constant elements. The geometry, the BEM discretization, and the boundary condition definitions are shown in Figure 5: notice that the temperature is in units of (K) and the heat transfer coefficient is in units of (W/m^2K). The endwall material is stainless steel with a constant thermal conductivity of $(k = 14.9W/m.K)$.

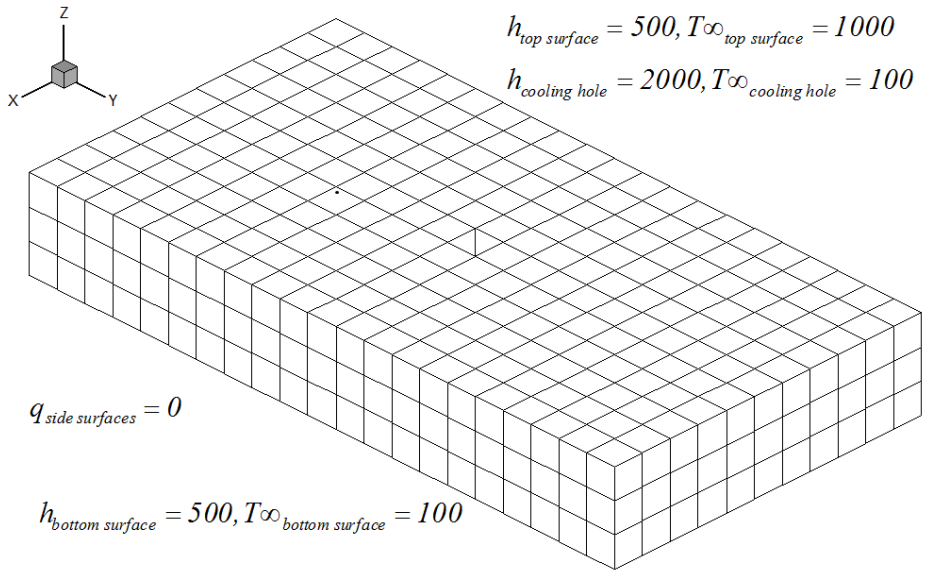

Figure 5: Geometry, BEM mesh, and boundary conditions used in solving the forward problem of a vertical square hole.

The discretized governing equations with the specified boundary conditions have been solved, and the temperature distribution is shown in the Figure 6, it can be seen that the temperature expands from $200K$ to $680K$.

The inverse problem had been solved just for the rectangular endwall without the square cooling hole in it, the same discretization was used in the direct problem is applied in the inverse problem which gives a total number of 654 constant elements; i.e. $((2\times11\times21)+(2\times11\times3)+(2\times21\times3))$. The boundary conditions along the sides of the endwall are adiabatic, whereas Cauchy conditions which were obtained from the direct solution are applied at the top and the bottom surfaces. The inlet and the exit surfaces of the cooling hole are set to an adiabatic boundary condition to ensure that all energy extracted by the cooling hole is captured by the sinks. In this case, the sinks are located at the geometrical center of the cooling hole. A distribution of three sinks were found to be a suitable number to have an optimized solution. An initial guess of the strength of sinks (Q_K) is set to be between -400 and zero (W/m^2) to begin the minimization process. The GA provided a global optimum for the strength of the three uniformly distributed sinks after 600 generations with a best fitness of 0.0725. Figure 7 shows the BEM discretization as well as the temperature contour plot field along the endwall.

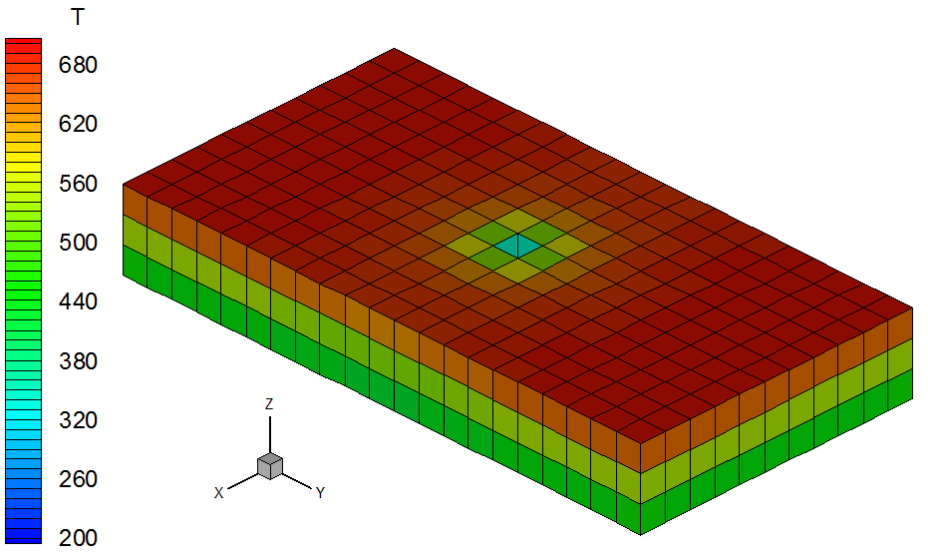

Figure 6: . Temperature distributions for the case of a vertical square cooling hole predicted by the BEM direct solution.

After the singularity strengths were optimized, the normal heat fluxes along the actual walls of the cooling hole were found in a post-processing stage by calculating heat flux vector components on internal points distributed along each side of the actual walls of the cooling hole. Because of problem symmetry, the GA predicted temperatures and heat fluxes can be compared to the direct solution along one side of the cooling hole. Figures 8 and 9 shows the BEM/GA reconstructed temperature and normal heat fluxes along one side/wall of the square cooling hole in comparison with the direct simulated temperature and normal heat fluxes. The results reveal good accuracy in predicting the temperature and heat flux distributions. It can be seen that a distribution of three singularities (sinks) is quite good to reconstruct heat flux distributions along the sides of the square cooling hole.

A typical convergence plot for the GA is provided below in Figure.

3.2 Results of the Inverse Problem for Circular Cooling Hole

For the case of the circular hole, a full conjugate heat transfer (CHT) model is developed to simulate the experimentally measured data at the exposed surfaces, which provides a numerical input for the inverse problem. The CHT model was simulated using the commercial CFD code Fluent version 6.1.22. In this case, the

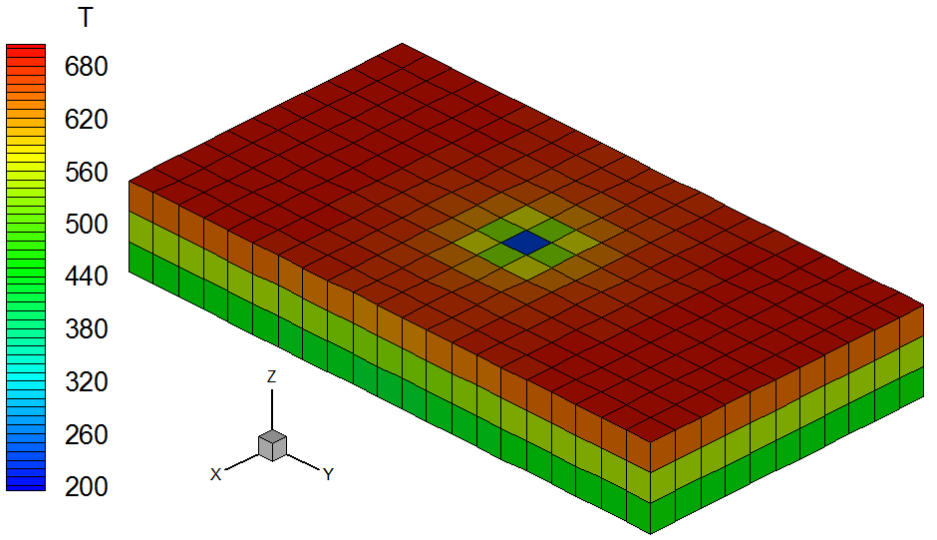

Figure 7: . BEM discretization and resulting temperature contour plot for the case of a vertical square cooling hole predicted by the inverse solution.

endwall dimensions are $((x = 50cm)\times(y = 3cm)\times(z = 9cm))$ with single circular cooling hole. The cooling hole has a diameter of $(D = 1cm)$ with an injection angle of 30 with the axial direction. Here, the conjugate heat transfer simulations were modeled using a linear model for the thermal conductivity $(k = 16.63\,W/m.K)$. Since the mesh for CHT model is different from the BEM mesh, the CHT simulated temperatures and heat fluxes were interpolated from the CHT mesh to BEM mesh using radial basis functions (RBF) interpolation with 20 points [Powell, (1992), Li and Chen (2002)]. The inverse problem is modeled using a discretization of 1254 constant elements; i.e. $((2\times50\times90)+(2\times50\times3)+(2\times9\times3))$. The CHT mesh and the BEM mesh are shown in Figure 10.

The inverse problem was solved using a distribution of 20 singularities (sinks). Those sinks were distributed along five lines such that there are four sinks per line. The optimum location of the lines were found to be one line at the geometrical center of the circular hole, whereas, the other four lines were located by offsetting the centerline by a distance of $(D/4)$ in the four sides, as shown in Figure 12. An initial guess of the strength of sinks (Q_K) is set to be between -200 and 200 (W/m^2) to begin the minimization process.

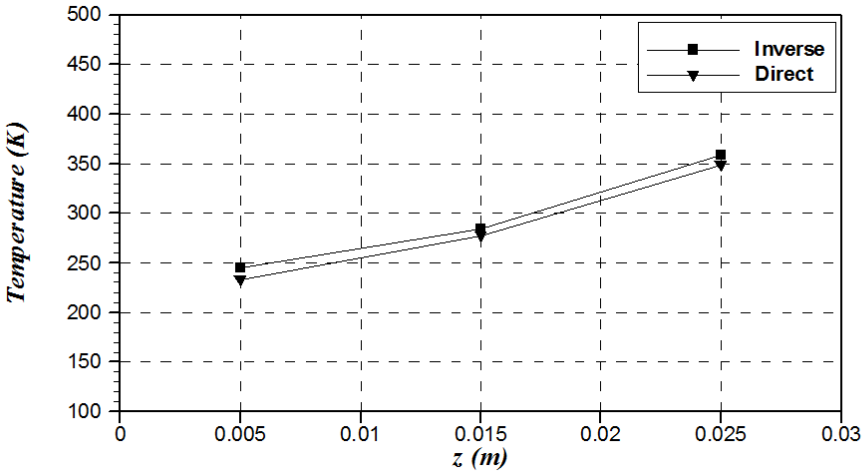

Figure 8: . Plot of GA predicted temperature compared to the direct simulated temperature along one side of the vertical square cooling hole.

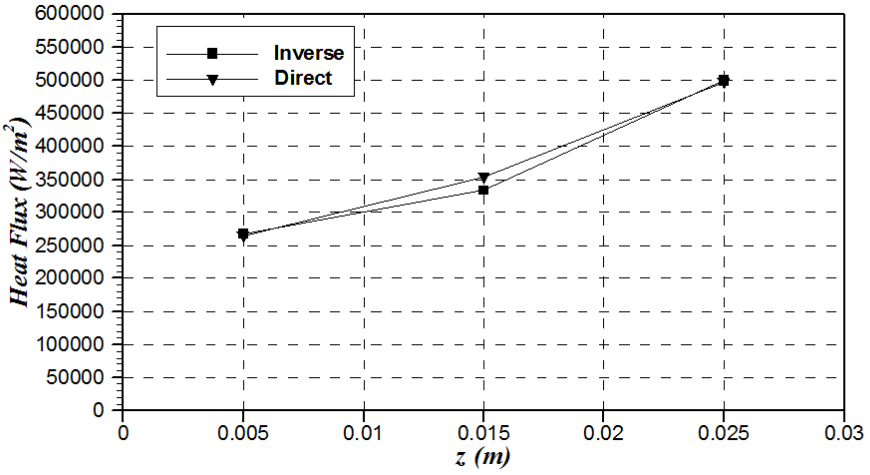

Figure 9: . Plot of the GA predicted heat flux compared to the direct simulated heat flux along one side of the vertical square cooling hole.

The GA provided a global optimum for the strength of the twenty uniformly distributed sinks after 2000 generations with a best fitness of 0.00156. Figure 13 shows a temperature contours predicted by both the CHT simulation as well as the

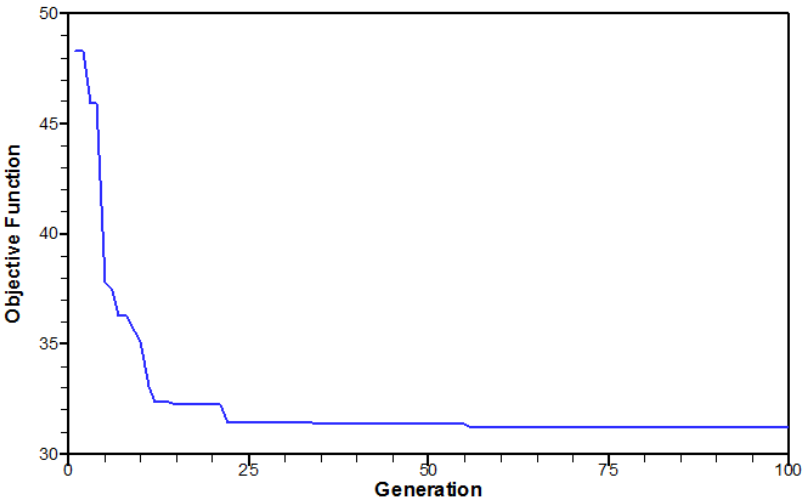

Figure 10: Convergence plot of the GA for the optimization of the singularity strenghts.

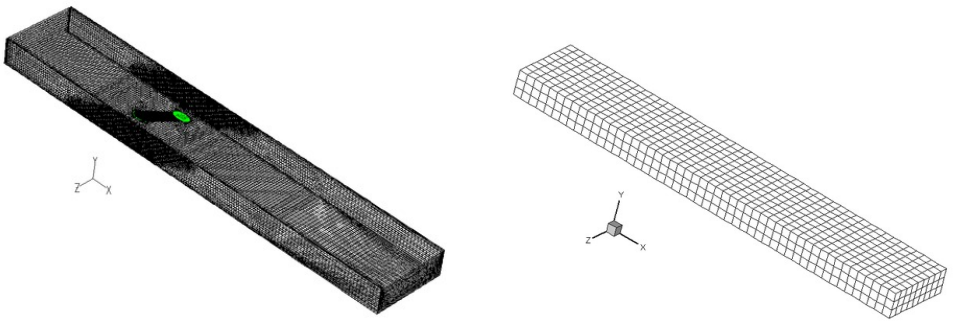

(a) CHT mesh (b) BEM mesh

Figure 11: . A plot of CHT mesh and the BEM mesh used for solving the circular cooling hole.

GA solution.

Again, after the singularity strengths were optimized, the normal heat fluxes along the actual walls of the cooling hole were found in a post-processing stage by calculating heat flux vector components on internal points distributed along each side of the actual walls of the cooling hole. In this case, the GA reconstructed temper-

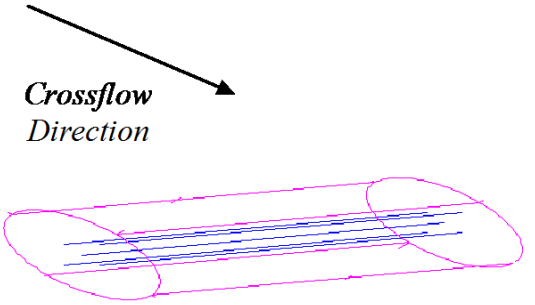

Figure 12: . Location of the 20 singularities (sinks) along the five lines (blue) used for solving the inverse problem of circular cooling hole.

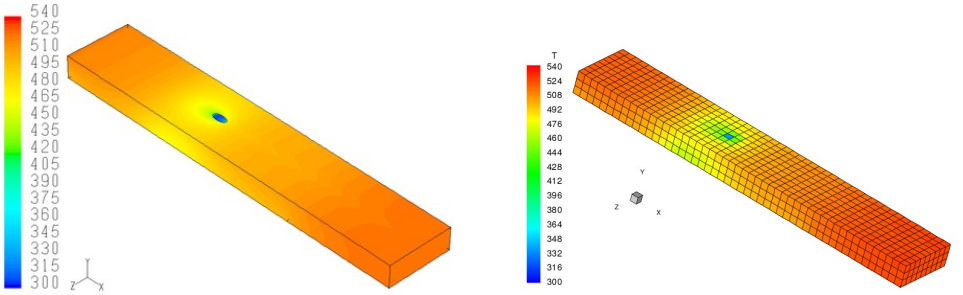

(a) CHT solution (b) GA solution

Figure 13: . A plot of the temperature contours predicted by both CHT and GA solutions for circular cooling hole.

atures and heat fluxes were compared to the CHT simulated ones along four lines; Line-1 through Line-4, located at the physical walls of the cooling hole as shown in Figure 14. Figures 15 and 16 shows the BEM/GA reconstructed temperature and normal heat fluxes along the four lines/edges of the circular cooling hole in comparison with the CHT simulated temperature and normal heat fluxes. The results reveal good accuracy in predicting the temperature and heat flux distributions. It can be seen that a distributions of twenty singularities (sinks) along five lines is good enough to reconstruct heat flux distributions along the sides of the circular cooling hole.

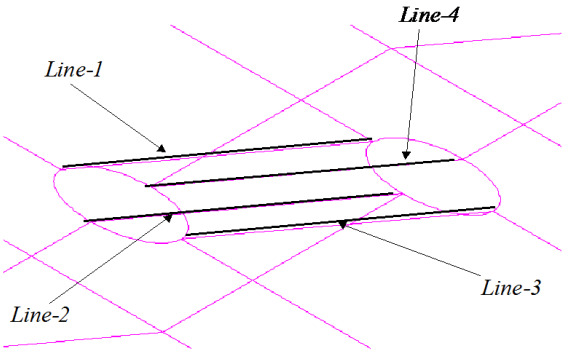

Figure 14: . Location of the four lines/edges used to compare the GA predicted results to the CHT simulated ones for the case of circular cooling hole.

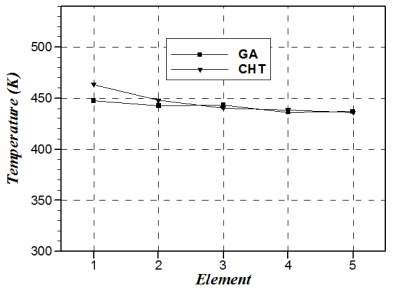

(a) Line-1

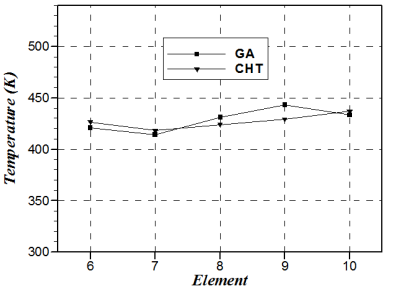

(b) Line-2

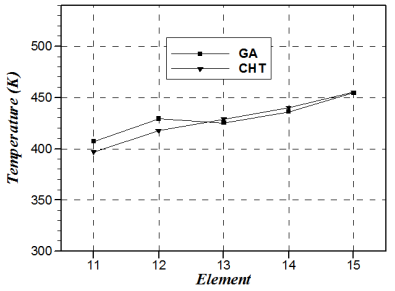

(c) Line-3

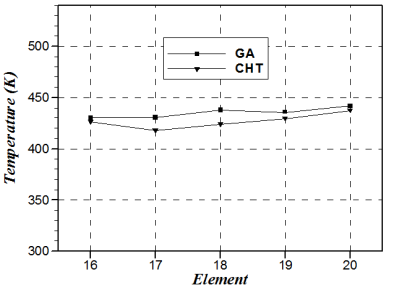

(d) Line-4

Figure 15: Plot of GA predicted temperature compared to the CHT simulated temperature along four lines for the case of circular cooling hole.

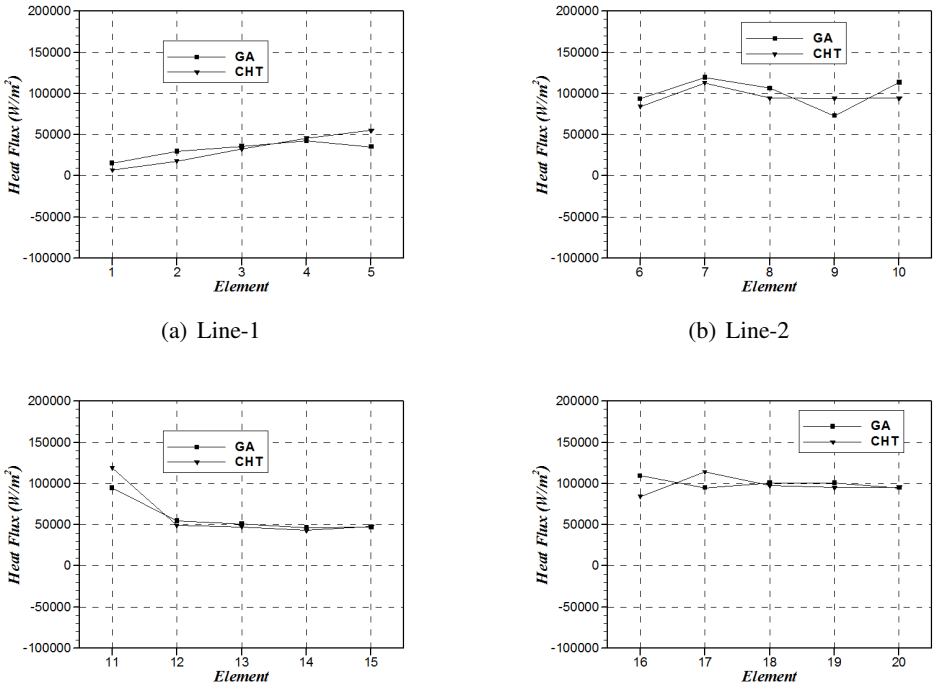

(a) Line-1 (b) Line-2

(c) Line-3 (d) Line-4

Figure 16: Plot of GA predicted temperature compared to the CHT simulated temperature along four lines for the case of circular cooling hole.

4 Conclusions

In this paper, a hybrid singularity superposition/boundary element-based inverse problem method for the reconstruction of 3D heat flux distributions was developed. Cauchy conditions are imposed at exposed surfaces while convective boundary conditions are unknown at surfaces that are not amenable to measurements. The purpose of the inverse analysis is to determine the heat flux distribution along edges/walls of the cooling holes. This is accomplished in an iterative process by distributing a set of singularities at the vicinity of the cooling hole surfaces along the cooling hole centerline with a given initial strength distribution. A forward steady-state heat conduction problem is solved using the boundary element method (BEM), and an objective function is defined to measure the difference between the heat flux measured at the exposed surfaces and the heat flux predicted by the BEM under the current strength distribution of the singularities. A GA iteratively alters

the strength distribution of the singularities until the measuring surfaces heat fluxes are matched, thus, satisfying Cauchy conditions. The hybrid singularity superposition/BEM approach thus eliminates the need to mesh the surfaces of the film cooling hole and the need to parametrize the heat flux over that surface. Rather, the heat flux is determined in a post-processing stage after the inverse problem is solved. The results provided validate the approach and reveal good accuracy between the BEM/GA predicted heat fluxes and the CHT simulated heat fluxes along the inaccessible cooling hole walls.

References

Divo, E., Kassab, A.J., Kapat, J.S., Chyu, M.K. (1999): Retrieval of Multidimensional Heat Transfer Coefficient Distributions Using an Inverse BEM-Based Regularized Algorithm: Numerical and Experimental Results, ASME-paper HTD-Vol. 364-1, Proceedings of the ASME, Heat Transfer Division, Witte, L. C.(Ed.), pp. 235-244.

Divo, E.A., Kassab, A.J. (2003): Boundary Element Method for Anisotropic Hetrogeneous Heat Conduction, Wessex Institute of Technology (WIT) Press, Southampton, UK, and Boston, USA.

Divo, E.A., Kassab, A.J., Rodriguez, F. (2003): Parallel Domain Decomposition Approach for large-scale 3D Boundary Element Models in Linear and Non-Linear Heat Conduction, Numerical Heat Transfer, Part B, Fundamentals, Vol. 44, No.5, pp. 417-437.

Divo, E., Kassab, A.J. (1997): A Boundary Integral Equation for Steady Heat Conduction in Anisotropic and Hetrogenous Media, Numerical Heat Transfer, Part B: fundamentals, Vol. 32, No. 1, pages 37-61.

Divo, E., Kassab, A.J., Rodrigues, F. (2003): An Efficient Singular Superposition Technique For Cavity Detection and Shape Optimization, Inverse Problems in Engineering Mechanics IV: international symposium on inverse problems in engineering mechanics, (ISIP 2003), Masataka Tanaka, (Ed.), Elsevier Press, 2003, pp. 241-250.

Divo, E., Kassab, A.J., Rodriguez, F. (2004): An Efficient Singular Superposition Technique For Cavity Detection and Shape Optimization, Numerical Heat Transfer, Part B: Fundamentals, Vol. 46, No. 1, 2004, pp.1-30.

Goldstein, R.J., Eckert, E.R.G., Ramsey, J.W. (1998): Film Cooling with Injection Through Holes: Adiabatic Wall Temperatures Downstream of a Circular Hole, ASME Journal of Engineering for Power, Vol. 90, pp. 384-395.

Goldstein, R.J., Eckert, E.R.G., Burggraf, F. (1974): Effects of Hole Geometry and Density on Three Dimensional Film Cooling, Int. J. of Heat and Mass Transfer, Vol. 17, 1974, pp. 595-607.

Goldstein, R.J. (1971): Advances in Heat Transfer, Vol. 7, pp. 321-379, Academic Press, New York.

Goldberg, D.E. (1989): Genetic Algorithms in Search, Optimization and Machine Learning, Addison-Wesley, Reading, MA.

Heselhaus, A., Vogel, D.T. (1995): Numerical Simulation of Turbine Blade Cooling with Respect to Blade Heat Conduction and Inlet Temperature Profiles, AIAA Paper No. 95-3041, 31st AIAA/ASME/SAE/ASEE Joint Propulsion, Conference and Exhibit, San Diego, California.

Kassab, A.J., Wrobel, L.C. (2000): Boundary Element Methods in Heat Conduction, Chapter 5 in Recent Advances in Numerical Heat Transfer, W.J. Mincowycz and E.M. Sparrow, (eds.), Vol. 2, Taylor and Francis, New York, pp. 143-188.

Kassab, A.J., Divo, E., Heidmann, J.D., Steinthorsson, E., Rodriguez, F. (2003): BEM/FVM Conjugate Heat Transfer Analysis of a Three-Dimensional Film Cooled Turbine Blade, International Journal for Numerical Methods in Heat Transfer and Fluid Flow, Vol. 13, No.5, 2003, pp. 581-610.

Kassab, A.J., Divo, E., Chyu, M. (1999): A BEM-Based Inverse Algorithm to Retrieve Multi -Dimensional Heat Transfer Coefficients from Transient Temperature Measurements, BETECH99, Proceedings of the 13th International Boundary Element Technology Conference, Las Vegas, Chen, C. S., Brebbia, C. A. and Pepper, D. (Eds), Computational Mechanics, Boston, Ma., pp. 65-74.

Kercher, D.M. (1998): A Film Cooling CFD Bibliography: 1971-1996, Int. J. of Rotating Machinery, Vol. 4, pp. 61-72.

Li, J., Chen, C.S. (2001): A Simple Efficient Algorithm for Interpolation Between Different Grids in Both 2D and 3D, Mathematics and Computers in Simulation, Vol. 58, No. 2, 2001, pp. 125-132.

Powell, M.J.D. (1992): The Theory of Radial Basis Function Approximation, Advances in Numerical Analysis, Vol. II, Light, W. (ed.), Oxford Science Publications.

Silieti, M., Divo, E., Kassab, A.J. (2004): The Effect of Conjugate Heat Transfer on Film Cooling Effectiveness, ASME-paper 2004-HT-FED-56234, Charlotte, North Carolina.

Silieti, M., Divo, E., Kassab, A.J. (2004): Numerical Investigation of Adiabatic and Conjugate Film Cooling Effectiveness on a Single Cylindrical Film Cooling Hole, ASME- paper No. IMECE2004-62196, Anaheim, California.

Silieti, M., Divo, E., Kassab, A.J. (2004): An Inverse BEM/GA Based Approach For Retrieval of Multi-Dimensional Heat Transfer Coefficients within Film Cooling Holes/Slots, BEM XXVI, Proc. of the 26th World Conf. on Boundary Elements and Other Mesh Reduction Methods, C.A. Brebbia (ed.), Wessex Institute of Technology, Southampton, UK, pp. 217-227.

Silieti, M., Divo, E., Kassab, A.J. (2009): An Inverse Boundary Element Method/Genetic Algorithm Based Approach for Retrieval of Multi-dimensional Heat Transfer Coefficients within Film Cooling Holes/Slots, Journal of Inverse Problems in Science and Engineering, Vol. 17, No. 3, 411-435.

Silieti, M., Divo, E., Kassab, A.J. (2004): Singular Superposition/BEM Inverse Technique for Reconstruction of Multi-dimensional Heat Flux Distributions with Application to Film Cooling Slots, ASME-paper No.IMECE 2004-62208, Anaheim, California.

Wrobel, L.C., Aliabadi, M.H. (2002): The Boundary Element Method: Applications in Thermo -Fluids and Acoustics, Vol 1, John Wiley and Sons, Inc, New York.

York, D.Y., Leylek, J.H. (2002): Leading Edge Film Cooling Physics: Part I - Adiabatic Effectiveness, ASME-paper GT-2002-30166, Amsterdam, The Netherlands.

York, D.Y., Leylek, J.H. (2002): Leading Edge Film Cooling Physics: Part II - Heat Transfer Coefficient, ASME-paper GT-2002-30167, Amsterdam, The Netherlands.

York, W.D., Leylek, J.H. (2003): Three-Dimensional Conjugate Heat Transfer Simulation of an Internally Cooled Gas Turbine Vane, ASME-paper 2003-GT-38551, Georgia.